WestVirginiaUniversity
THE RESEARCH REPOSITORY @ WVU

Faculty Scholarship

1994

Tracking unstable periodic orbits in the Belousov-Zhabotinsky reaction

Valery Petrov

Michael J. Crowley

Kenneth Showalter

Follow this and additional works at: https://researchrepository.wvu.edu/faculty_publications

Digital Commons Citation

Petrov, Valery; Crowley, Michael J.; and Showalter, Kenneth, "Tracking unstable periodic orbits in the Belousov-Zhabotinsky reaction" (1994). *Faculty Scholarship*. 413.
https://researchrepository.wvu.edu/faculty_publications/413

This Article is brought to you for free and open access by The Research Repository @ WVU. It has been accepted for inclusion in Faculty Scholarship by an authorized administrator of The Research Repository @ WVU. For more information, please contact ian.harmon@mail.wvu.edu.

Tracking Unstable Periodic Orbits in the Belousov-Zhabotinsky Reaction

Valery Petrov, Michael J. Crowley, and Kenneth Showalter
Department of Chemistry, West Virginia University, Morgantown, West Virginia 26506-6045
(Received 20 December 1993)

An adaptive control algorithm for tracking unstable periodic orbits is presented. Automatic tracking is made possible by incorporating a stability-analysis subroutine into a map-based control scheme. The method is used to track unstable orbits in the Belousov-Zhabotinsky reaction.

PACS numbers: 82.40.Bj, 05.45.+b

Dynamical systems are typically characterized by systematic measurements of their asymptotic behavior as a function of a system parameter. The resulting constraint-response diagram provides insights into the system's bifurcation structure, i.e., the bifurcations that underlie the changes in qualitative dynamical behavior [1]. Successively varying other system parameters generates additional bifurcation diagrams, allowing the construction of phase diagrams of the behavior. Such measurements provide information about the *stable states* of a system. If an accurate model exists, a more detailed picture of the dynamics—including information about the *unstable states*—can be developed through the use of continuation methods [2].

A different approach for characterizing dynamical systems has become possible with newly developed techniques for stabilizing unstable periodic orbits in experimental systems, such as the Ott-Grebogi-Yorke (OGY) method [3,4] and related map-based schemes [5–7]. These control algorithms permit the stabilization of unstable states without relying on model descriptions. By tracking the unstable states and combining the measurements with measurements of the stable states, features of the bifurcation structure of a system can be determined before any modeling studies are carried out.

The first experiments on tracking unstable states were carried out using electronic and laser systems. Carroll *et al.* [8] reported tracking unstable periodic orbits in a chaotic Duffing circuit, and Gills *et al.* [9] reported tracking unstable stationary states in a chaotic multimode laser in which the range of stable lasing was significantly extended.

We present a new tracking algorithm, which determines the stability properties as well as the location of the unstable states. Automatic tracking is made possible by incorporating a stability-analysis subroutine into a map-based control scheme [5,6]. The procedure is tested in an experimental setting by tracking unstable periodic orbits in the Belousov-Zhabotinsky (BZ) reaction as a laboratory control parameter is varied. The experimental methods of previous control experiments, where periodic orbits were targeted and stabilized within the chaotic regime of the BZ reaction [10], serve as the basis for the tracking experiments reported here.

Tracking procedures offer new possibilities for control and characterization of dynamical systems. As in previous control methods [3–7], only tiny perturbations are necessary to stabilize a particular unstable state; hence, the states are representative of the original autonomous system. Tracking allows the stabilization of unstable states outside the chaotic regime, as a particular state can be followed through a complete bifurcation sequence —from the point where it becomes unstable to the point where it regains stability. In addition, as an unstable periodic orbit is tracked the Floquet multiplier (in the unstable direction) can be automatically determined by the stability-analysis subroutine described below.

The map-based control method is appropriate for stabilizing periodic orbits in low-dimensional, highly dissipative chaotic systems [5,6]. Rather than targeting the stable manifold of the fixed point in the Poincaré section as in the OGY algorithm [3,4], the method is based on targeting the fixed point directly in the 1D return map. For systems described by effectively 1D maps, the behavior in the local vicinity of a fixed point obeys linear dynamics according to the map

$$X_{n+1}=\lambda(X_n-X_F)+X_F\,, \tag{1}$$

where X_n is the value of the measured observable on the nth iteration, X_F is the fixed point, and λ is its Floquet multiplier. We assume there is an experimentally accessible parameter, p, which alters the dynamics in such a way that the fixed point moves in the direction of the unstable manifold when a small perturbation, δp, is applied. Following the application of such a perturbation, the system evolves according to the position of the shifted fixed point,

$$X_F(p+\delta p)=X_F(p)+\frac{\partial X_F}{\partial p}\delta p\,. \tag{2}$$

A particular unstable fixed point, X_F, is stabilized by determining the perturbation δp such that the next return, $X_{n+1}(p+\delta p)$, is equal to $X_F(p)$. The appropriate δp is simply proportional to the deviation of the system from X_F,

$$\delta p=K_0[X_n-X_F(p)]\,, \tag{3}$$

where the proportionality factor,

$$K_0=\frac{\lambda}{(\lambda-1)\,\partial X_F/\partial p}\,, \tag{4}$$

© 1994 The American Physical Society

is determined in advance from the horizontal shift of the return map resulting from the perturbation δp [5]. Perfect control would occur—if there were no measurement or targeting errors—with all X near X_F mapping to X_F, and the system in the local region of X_F would be described by a new map of zero slope [6].

Control is also possible for other values of the proportionality constant, K_S. For any value of K_S applied during control, the system evolves within the linear region of X_F according to

$$X_{n+1}=S(X_n-X_F)+X_F\,, \tag{5}$$

where the local slope S of the new map is related to K_S by

$$S=\lambda+\frac{\partial X_F}{\partial p}K_S(1-\lambda)\,. \tag{6}$$

Thus, the fixed point is stabilized for any K_S that produces a slope S with magnitude less than unity, or, conversely, the multiplier S of the fixed point under control can be set to any value by the appropriate choice of K_S. This relationship allows the values of S, K_S, and λ to be determined while the unstable fixed point remains under control.

It is first necessary to initialize the tracking procedure, i.e., locate and stabilize a desired unstable orbit at some value of the bifurcation parameter q. (We distinguish between the control parameter p and bifurcation parameter q because they need not be the same.) The starting point can be located either in the vicinity of a bifurcation that destabilizes the periodic orbit, or in chaos, where the evolution of the system ensures that the local vicinity of the fixed point will be visited. In both cases, the location of the fixed point and value of the Floquet multiplier can be readily determined.

Tracking X_F through changes in the bifurcation parameter requires adaptive control, where the values of X_F and K_0 must be redetermined without the system leaving the local vicinity of X_F (where the control algorithm is effective). The control algorithm is continuously applied throughout the change in q in order to maintain control. Provided the change from q to $q'=q+\delta q$ is sufficiently small, the new X_F and λ are close to the previous values and linear behavior around the fixed point can be assumed. The value $K_0(q)$ and $X_F(q)$ used in the previous step, however, will be incorrect for convergence to the new $X_F(q')$. Consider the effect of using $K_0(q)$ and $X_F(q)$ in Eq. (3) for the system at q'. With these values, the system will converge to a point that is distinct from both the old $X_F(q)$ and the new $X_F(q')$. It can be shown that if the convergence is to the value $X^*(q')$, the value of $X_F(q')$ is given by

$$X_F(q')=\frac{X^*(q')-\lambda(q)X_F(q)}{1-\lambda(q)}\,, \tag{7}$$

where the values of $X_F(q)$ and $\lambda(q)$ are known from the previous step.

With the new fixed point known, the next step is to determine the appropriate value of the proportionality constant for the control algorithm, $K_0(q')$, and the new multiplier, $\lambda(q')$. One could determine the value of λ by switching off control and simply allowing the system to diverge; in experimental settings, however, this approach often fails because the system leaves the linear region of the fixed point too quickly, especially for highly unstable orbits. A systematic method for determining the new K_0 and λ utilizes the relationship given by Eq. (6). The proportionality constant K_S is first set to a value, K_1, that will produce a slightly unstable fixed point, e.g., with $|S|\approx 1.5$. The divergence from X_F is mild, allowing enough returns to the section for an accurate determination of the slope S_1. Before the system has diverged beyond the linear control range, K_S is changed to a new value, K_2, which corresponds to a mildly stable fixed point, e.g., with $|S|\approx 0.6$. The system will slowly converge back to X_F and the slope, S_2, is determined. The experimental measurements during the divergence/convergence scheme are then used with Eqs. (4) and (6) to yield

$$K_0=\frac{S_2K_1-S_1K_2}{S_2-S_1} \tag{8}$$

and

$$\lambda=\frac{S_2K_1-S_1K_2}{K_1-K_2}\,. \tag{9}$$

These steps, redetermining X_F and finding the corresponding values K_0 and λ from the stability analysis, can be reiterated in each step of the tracking until satisfactory convergence is achieved.

We now demonstrate the tracking algorithm with the Belousov-Zhabotinsky reaction in a continuous-flow, stirred tank reactor (CSTR). This system displays a variety of dynamical responses, including period-doubling cascades to chaos [11] and complex mixtures of mixed-mode oscillations and chaos [12,13]. The procedure will first be illustrated with the Györgyi-Field [14] model of the BZ reaction, with the parameters similar to those used in the experimental system. A typical bifurcation diagram of this model is shown in Fig. 1(a), where a period-doubling sequence from period-1 oscillations to chaos is followed by the reverse sequence to simple period 1. The period-1 orbit loses stability at the first period-doubling bifurcation; the locus of the unstable orbit, however, is readily determined by the tracking procedure. The open circles show the location of the stabilized orbit at each incremental increase in the bifurcation parameter q (the reciprocal residence time). The corresponding locus, shown by the solid line, was determined by the path-following algorithm AUTO [2]. The Floquet multiplier for the period-1 orbit, calculated from Eq. (9), is shown as a function of q by the open circles in Fig. 1(b). The values calculated from AUTO are shown by the solid line.

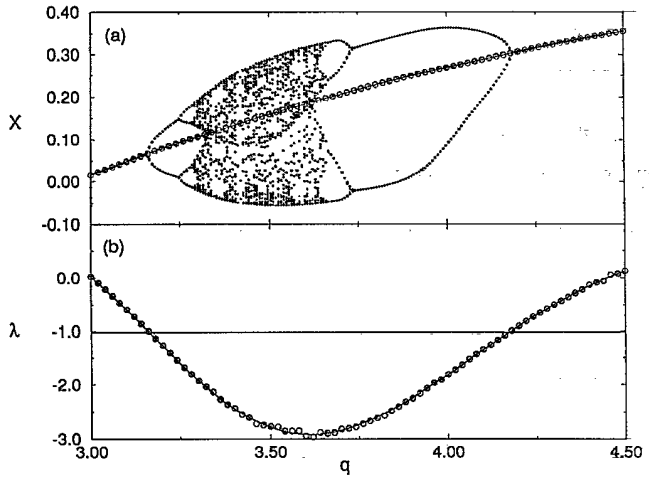

FIG. 1. Period-doubling sequence calculated from the three-variable Györgyi-Field [14] model of the Belousov-Zhabotinsky reaction. (a) Bifurcation diagram showing maximum in oscillations (●) of variable $X=\log_{10}([\mathrm{Ce(IV)}]\xi)$ as a function of the bifurcation parameter $q=1/10^{-4}\tau$, where ξ is a scaling constant and τ is the residence time. The open circles show the locus of the unstable period-1 orbit. (b) Values of period-1 Floquet multiplier as a function of q. The parameters used in the calculation are the same as in Ref. [14] except [malonic acid] $=0.26M$.

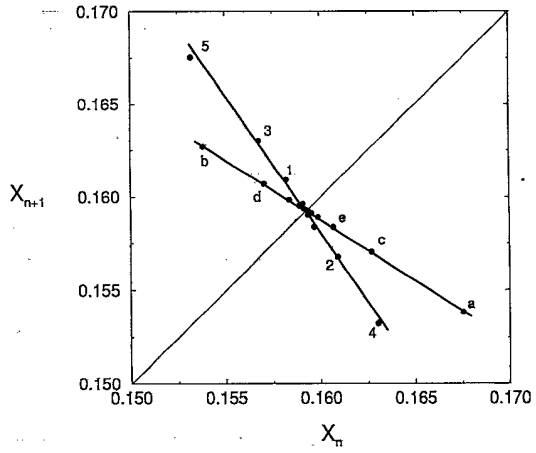

FIG. 2. Return map showing linear dynamics under control for two different values of K in the vicinity of the period-1 fixed point. The proportionality constant was first set to $K_1=8.369\times10^{-4}$ and then to $K_2=1.460\times10^{-3}$. The corresponding values of S_1 and S_2 in Eqs. (8) and (9) yield the values $K_0=1.915\times10^{-3}$ and $\lambda=-2.766$ for the tracking step at $q=3.5$ in Fig. 1.

Each step of the tracking consisted of determining the new fixed point according to Eq. (7) followed by the stability analysis according to Eqs. (8) and (9). An example of the stability analysis for one step of the tracking in Fig. 1 is shown in Fig. 2. The value of K is first set to K_1 to generate a slope $S_1\approx-1.5$, and the system diverges away from the fixed point (values 1,2,3,...). After sampling 5 points, the value of K is changed to K_2 to give a slope $S_2\approx-0.6$. The system converges back to the fixed point, generating another 5 points (values $a,b,c,\ldots$). Least-squares fits of each set of points allow the accurate determination of the slopes, $S_1=-1.557$ and $S_2=-0.6571$, which are then used in Eqs. (8) and (9) to calculate values of K_0 and λ corresponding to the value of the bifurcation parameter q. The updated K_0 and λ are used in the next step of the tracking in determining the new value of X_F.

An application of the tracking algorithm to the experimental system is shown in Fig. 3. The BZ reaction was carried out in a continuous-flow, stirred tank reactor (volume=60.0 ml, stirring rate=2700 rpm) maintained at 28.0 ± 0.1 °C. Two computer-regulated syringe pumps were used, with malonic acid solution delivered by one and cerium and bromate solutions (acidified with sulfuric acid) delivered by the other. The period-1 orbit was tracked from $q=0.452$ through the period-doubling, chaos, and period-halving sequences to $q=0.422$. The tracking was automatically carried out by a laboratory computer—collecting the data, executing the algorithm, and controlling the pumps. The period-doubling sequence to chaos and the reverse sequence are similar to the calculated sequences in Fig. 1; however, some qualitative differences are apparent. These are mainly due to monitoring a different system variable and using a slightly different bifurcation parameter in the experiments. The potential of a bromide selective electrode, giving the effective bromide ion concentration, was used to monitor the system. The bifurcation parameter q was the flow

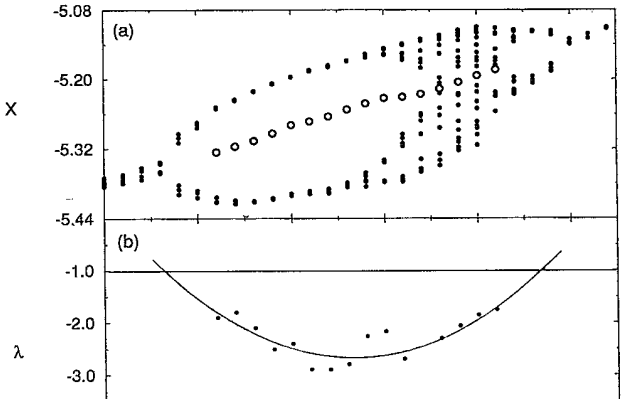

FIG. 3. Stable states (●) and tracked unstable period-1 orbit (○) of the BZ reaction as a function of bifurcation parameter q. The variable $X=\log_{10}[\mathrm{Br}^-]$ on crossing a Poincaré section defined by $X=-5.66$ in the X_t, $X_{t+\tau}$ phase plane ($\tau=12$ s). Feedstream concentrations (before mixing) and flow rates: [malonic acid] $=0.222M$ at 0.444 mL/min; $[\mathrm{Ce_2(SO_4)_3}]=4.50\times10^{-4}M$, $[\mathrm{NaBrO_3}]=0.102M$, and $[\mathrm{H_2SO_4}]=0.300M$ varied at q mL/min.

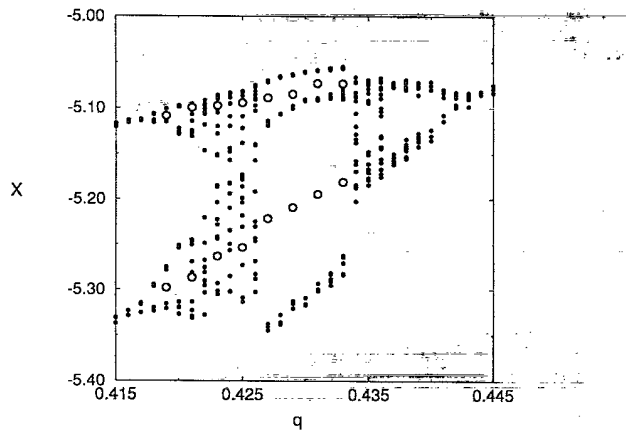

FIG. 4. Stable states (●) and tracked unstable period-2 orbit (○) in the BZ reaction. The monitored variable X and the bifurcation parameter q are the same as in Fig. 3 except the constant flow rate of the malonic acid solution was 0.440 mL/min.

rate of the Ce(III), bromate, and sulfuric acid feed streams (with the malonic acid flow rate held constant) [10]. The reactor residence time served as the perturbation parameter p.

Perturbations were applied during the first 25 s of each ~100 s cycle to stabilize and track the period-1 orbit, shown in Fig. 3(a) by the open circles. The experimentally determined values for the period-1 Floquet multiplier as a function of q are shown in Fig. 3(b). Although there is significant scatter in the values of λ due to experimental fluctuations (from flow rate variations, etc.), the qualitative features of the dependence on q are similar to the modeling calculations shown in Fig. 1(b).

Figure 4 shows an example of tracking period 2 through a period-doubling cascade that gives rise to 2:1 mixed-mode oscillations (two large amplitude and one small amplitude oscillations per cycle [12,13]). Period-2 oscillations were stabilized after the period-doubling bifurcation at $q=0.419$ and tracked through chaos and the mixed-mode oscillations to $q=0.433$. The stabilization algorithm was robust and most effective when the perturbation was applied 80 s after crossing the Poincaré section, with a duration of 40 s, or about $\frac{1}{5}$ of the period.

The simplicity of map-based control methods offers significant advantages for the implementation of efficient tracking schemes. Linear map dynamics can also be used to stabilize and track stationary states. The temporal evolution of a two-variable system in the local vicinity of a focus stationary state is described by

$$X(t)=X_F+C\exp(\alpha t)\sin(\omega t+\varphi)\,, \tag{10}$$

where α is the real part and ω is the imaginary part of the eigenvalue. The exponential growth of $X(t)$ is modulated by sinusoidal oscillations, where the minima and maxima in X are equally spaced in time by $\Delta t=\pi/\omega$. The appearance of the extrema in the linear region of X is subject to the recursion law

$$X_{i+1}-X_F=\lambda(X_i-X_F)\,, \tag{11}$$

where X_{i+1} and X_i are the successive values and $\lambda=-\exp(\alpha\pi/\omega)$. The linear dynamics of the system near the stationary state can therefore be represented by a 1D map and the tracking algorithm can be easily applied. We report elsewhere [15] on stabilizing steady flame fronts through the chaotic regime of laminar combustion.

We thank the National Science Foundation (Grant No. CHE-9222616) for supporting this research. Acknowledgement is made to the donors of The Petroleum Research Fund, administered by the American Chemical Society, for partial support of this research.

[1] J. Guckenheimer and P. Holmes, *Nonlinear Oscillations, Dynamical Systems, and Bifurcations of Vector Fields* (Springer-Verlag, New York, 1983).
[2] E. J. Doedel, Congress Num. **30**, 265 (1981); E. J. Doedel and J. P. Kernevez, *AUTO: Software for Continuation and Bifurcation Problems in Ordinary Differential Equations* (Applied Mathematics, California Institute of Technology, Pasadena, 1986).
[3] E. Ott, C. Grebogi, and J. A. Yorke, Phys. Rev. Lett. **64**, 1196 (1990).
[4] T. Shinbrot, C. Grebogi, E. Ott, and J. A. Yorke, Nature (London) **363**, 411 (1993).
[5] B. Peng, V. Petrov, and K. Showalter, J. Phys. Chem. **95**, 4957 (1991).
[6] V. Petrov, B. Peng, and K. Showalter, J. Chem. Phys. **96**, 7506 (1992).
[7] R. W. Rollins, P. Parmananda, and P. Sherard, Phys. Rev. E **47**, R780 (1993).
[8] T. Carroll, I. Triandaf, I. B. Schwartz, and L. Pecora, Phys. Rev. A **46**, 6189 (1992).
[9] Z. Gills, C. Iwata, R. Roy, I. B. Schwartz, and I. Triandaf, Phys. Rev. Lett. **69**, 3169 (1992).
[10] V. Petrov, V. Gáspár, J. Masere, and K. Showalter, Nature (London) **361**, 240 (1993).
[11] R. H. Simoyi, A. Wolf, and H. L. Swinney, Phys. Rev. Lett. **49**, 245 (1982).
[12] R. A. Schmitz, K. R. Graziani, and J. L. Hudson, J. Chem. Phys. **67**, 3040 (1977).
[13] V. Petrov, S. K. Scott, and K. Showalter, J. Chem. Phys. **97**, 6191 (1992).
[14] L. Györgyi and R. J. Field, Nature (London) **355**, 808 (1992).
[15] V. Petrov, M. Crowley, and K. Showalter, J. Chem. Phys. (to be published).